Polymer 49 (2008) 3477–3485

Contents lists available at ScienceDirect

Polymer

journal homepage: www.elsevier.com/locate/polymer

Folate-encoded and Fe_3O_4-loaded polymeric micelles for dual targeting of cancer cells

Xiaoqiang Yang [a,1], Yinghua Chen [b,1], Renxu Yuan [a], Guihua Chen [b], Elvin Blanco [c], Jinming Gao [c], Xintao Shuai [a,*]

[a] BME Center, State Key Laboratory of Optoelectronic Materials and Technologies, School of Chemistry and Chemical Engineering, Sun Yat-Sen University, Guangzhou 510275, PR China
[b] The Third Affiliated Hospital, Sun Yat-Sen University, Guangzhou 510630, PR China
[c] Simmons Comprehensive Cancer Center, University of Texas Southwestern Medical Center at Dallas, Dallas, TX 75390, USA

ARTICLE INFO

Article history:
Received 11 March 2008
Received in revised form 4 June 2008
Accepted 5 June 2008
Available online 11 June 2008

Keywords:
Micelles
Block copolymers
Drug delivery

ABSTRACT

Diblock copolymers of poly(ethylene glycol) (PEG) and poly(ε-caprolactone) (PCL) bearing a tumor-targeting ligand, folate, were self-assembled into micelles. Superparamagnetic iron oxide (SPIO) nanoparticles and an anticancer drug doxorubicin (DOX) were coencapsulated within the micelles less than 100 nm in diameters. These SPIO–DOX-loaded micelles were superparamagnetic at room temperature, but turned ferrimagnetic at 10 K, consistent with magnetic properties of primary SPIO nanoparticles. Cell culture experiments demonstrated the potential of these polymeric micelles as an effective dual targeting nanoplatform for the delivery of anticancer drugs. Folate attachment to micelles resulted in the recognition of the micelles by tumor cells over-expressing folate receptors, leading to facilitation in cellular uptake of micelles, and the transport efficiency of the SPIO-loaded and folate-functionalized micelles into the tumor cells can be further enhanced by applying an external magnetic field to the cells.

1. Introduction

Over the past decades, polymeric micelles have drawn considerable interests because of their great potential in anticancer drug delivery and diagnostic imaging applications [1–4]. These nano-sized particles, formed from the self-assembly of amphiphilic block copolymers, provide a unique core–shell architecture wherein the hydrophobic core serves as a natural carrier environment for hydrophobic drugs or imaging agents while the hydrophilic shell enables particle stabilization in aqueous solutions [5–7]. Despite of their numerous advantages such as drug solubilization and prolonged blood circulation, micelles lack the ability to achieve high targeting efficiency at tumor sites. Moreover, insufficient cell uptake further decreases the therapeutic efficacy of the administered drug, and nonspecific accumulation in healthy tissues leads to serious side effects and limits the dosage that can be administered. Hence, studies involving means to further improve the tumor specificity of micelles in therapeutic and diagnostic applications are a growing trend in micellar research. A well-known strategy to achieve active tumor targeting is to encode the micellar outer layer with specific ligands that can recognize molecular signatures on the cancer cell surface. Targeting ligands that can serve such a purpose include folic acid, peptides such as cyclic (Arg-Gly-Asp-D-Phe-Lys) (cRGD), transferrin and monoclonal antibodies [8–11]. However, in order for the nanoparticles to be able to recognize cell surface receptors, they need to be directed to tumor sites in the first place. Therefore, an external targeting strategy, such as a guided magnetic field, which can hold the micelles in and/or effectively drive the micelles into tumor tissues is expected to improve drug delivery efficiency. Pioneering work in the area of external magnetic field-aided drug delivery dates back to the late 1970s, when Widder et al. developed the first magnetic microsphere as a drug carrier and used an external magnetic field to guide the drug/carrier to the targeted site [12,13]. Following this groundbreaking work, research on tumor targeted chemotherapy with magnetic nanoparticles has increased considerably over the past two decades [14–17]. Despite various advances, major success in drug targeting has been limited when compared to the application of magnetic particles as diagnostic contrast agents in magnetic resonance imaging (MRI) [18–20]. Further development and testing of novel magnetic carriers are necessary to achieve the therapeutic potential of magnetic targeting. Although regarded as a promising class of drug delivery vehicles, polymeric micelles combining dual magnetic and

* Corresponding author. Tel.: +86 20 84110365; fax: +86 20 84112245.
E-mail address: shuaixt@mail.sysu.edu.cn (X. Shuai).
[1] These authors contributed equally to this work.

0032-3861/$ – see front matter © 2008 Elsevier Ltd. All rights reserved.
doi:10.1016/j.polymer.2008.06.005

molecular targeting functions to tumor tissues and associated cells have rarely been exploited.

In this article, we describe dual targeting micelles that contain a molecular targeting ligand on the micelle surface as well as a cluster of superparamagnetic iron oxide (SPIO) nanoparticles in the cores for magnetic targeting. Micelles based on copolymers of poly(ε-caprolactone) (PCL) and poly(ethylene glycol) (PEG) bearing folate on the PEG distal ends, denoted as folate–PEG–PCL, were used to encapsulate the anticancer drug doxorubicin (DOX) and SPIO, after which cell culture experiments were conducted as a proof of concept to demonstrate their potential as a dual targeting system that can transport anticancer drugs to tumor cells effectively.

2. Experimental section

2.1. Materials

Phenyl ether (99%), benzyl ether (99%), 1,2-hexadecanediol (97%), oleic acid (99%), oleylamine (>70%) and iron(III) acetylacetonate were purchased from Sigma–Aldrich and used without further purification. Doxorubicin hydrochloride (DOX) was supplied by Shenzhen Main Luck Pharmaceutical Inc., Shenzhen, China, and was used as-received. MTT (3-(4,5-dimethylthiazol-2-yl)-2,5-diphenyltetrazolium bromide) was purchased from Sigma–Aldrich. RPMI-1640 medium, Dulbecco's phosphate-buffered saline (PBS), and 0.25% trypsin were purchased from Gibco BRL. All other chemicals used in experiments were of analytical grade, and used without further purification. A KB cell line derived from human oral cavity squamous carcinoma was obtained from the center of experimental animal, Sun Yat-sen University.

2.2. Synthesis of copolymers and Fe_3O_4 nanoparticles

The targeting and non-targeting copolymers, folate–PEG–PCL and allyl-PEG–PCL, were synthesized via multistep synthesis as described in our recent publication [21]. Fe_3O_4 nanoparticles (SPIO) were synthesized according to a reported method [22]. Briefly, iron(III) acetylacetonate (2 mmol), 1,2-hexadecanediol (10 mmol), oleic acid (6 mmol), oleylamine (6 mmol), and benzyl ether (20 mL) were mixed and magnetically stirred under a flow of nitrogen. The mixture was heated to 200 °C for 2 h and then, under a blanket of nitrogen, heated to reflux (300 °C) for 1 h. The black-colored mixture was cooled to room temperature by removing the heat source. The product, 6 nm Fe_3O_4 nanoparticles, was then precipitated with ethanol, centrifuged (6000 rpm, 10 min) to remove the solvent, and re-dispersed into hexane. A black-brown hexane dispersion of 6 nm Fe_3O_4 nanoparticles was then produced.

2.3. Preparation of SPIO–DOX-loaded micelles

SPIO and DOX-encapsulated micelles were prepared via the dialysis method. Briefly, 10 mg of folate–PEG–PCL, 2 mg of doxorubicin hydrochloride, triethylamine (1.3 mL), and SPIO (1.5 mg) were dissolved in a mixed solvent consisting of THF (1 mL) and DMSO (1 mL). The above solution was slowly added into 5 mL of deionized water under sonication using an UP 50H Dismembrator (Hielscher, Germany) and then dialyzed against deionized water for 2 days to allow the formation of SPIO–DOX-loaded micelles and to remove organic solvents and unencapsulated DOX dissolved in aqueous solution (M_w cut-off: 14,000 Da). Afterwards, the micelle solution was removed from the dialysis bag and filtered through a 0.22 μm membrane to remove large aggregates.

2.4. Micelle size and morphology

Micelles obtained were characterized with photon correlation spectroscopy, performed at 25 °C on a BI-200 SM dynamic laser scattering system from Brookhaven Instruments. Scattered light was detected at a 90° angle and collected on an autocorrelator. Sizes given are the means of five runs ± standard deviation. Samples for transmission electron microscopy (TEM, JEM-2010HR, Japan) analysis were prepared by drying a dispersion of the particles on a copper grid coated with amorphous carbon. Subsequently, a small drop of phosphotungstic acid (PTA) solution (2 wt.% in water) was added to the copper grid, and after 30 s the grid was blotted with filter paper for TEM observation.

2.5. Determination of DOX and SPIO-loading contents

The DOX-loading content (DLC), defined as the weight percentage of DOX in micelles, was quantified by UV–vis analysis using a Unico UV-2000 UV–vis spectrophotometer. First, DOX–SPIO-loaded micelle solutions were lyophilized to yield the solid micelle samples. Then the dried micelle samples were weighed and re-dissolved in a mixture of chloroform and DMSO (1:1, v/v). After the insoluble SPIO particles were removed from the solution by magnetic field-guided accumulation, the absorbance of DOX at 480 nm was measured to determine drug content in the solution using a previously established calibration curve. The loading density of SPIO inside polymeric micelles was determined using a polarized Zeeman Atomic Absorption Spectrophtotometer (Model: Z-2000 series). Briefly, the freeze-dried micelles were weighed and then added into 1 M HCl solution to allow the disaggregation of micelles and complete dissolution of SPIO crystals. Iron concentration was determined at the specific Fe absorption wavelength (248.3 nm) based on a previously established calibration curve. SPIO loading density was calculated as the ratio of iron oxide over the total weight of micelles.

2.6. Release of DOX from micelles

Freeze-dried micelle samples were resuspended in PBS (pH 7.4) or sodium acetate buffered solution (pH 5.0) and then transferred into a dialysis bag (M_w cut-off: 14,000 Da). The bag was placed into the same buffered solution (25 mL). The release study was performed at 37 °C in a Shanghai Yiheng Scientific DKZ incubator shaker. At selected time intervals, solution outside of the dialysis bag was removed for UV–vis analysis and replaced with fresh buffer solution. DOX concentration was calculated based on the absorbance intensity of DOX at 480 nm. In the assessment of drug release behavior, the cumulative amount of released drug was calculated, and the percentages of drug released from micelles were plotted against time. Release of free DOX (initial DOX concentration in dialysis bag: 40 μg/mL) from the dialysis bag at different pHs was performed as controls following the same procedure as described above.

2.7. Magnetic properties of SPIO–DOX-micelles

The magnetization data of SPIO and SPIO–DOX-loaded micelles were determined using a MPMS XL-7 Quantum Design SQUID magnetometer at 10 K and 300 K. Temperature control is achieved by the components within the Temperature Control Module (TCM) under the active control of the Model 1822 Controller and the control system software. The applied magnetic field was varied from 2×10^4 Oe to -2×10^4 Oe in order to generate hysteresis loops. The magnetic responsiveness of SPIO nanoparticles and SPIO–DOX-micelles in solution was tested by simply placing a magnet near the glass vial. A cylindrical sintered N-35 Nd–Fe–B

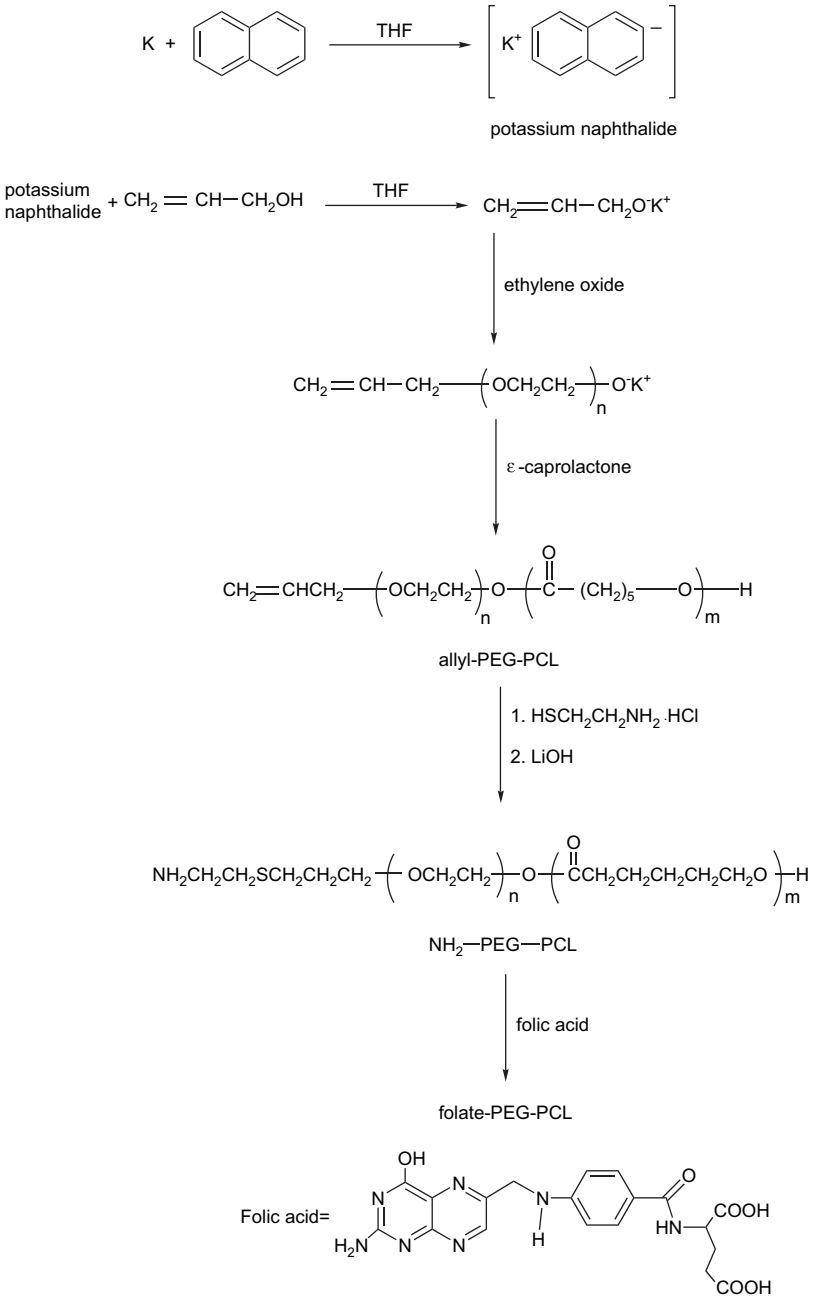

Scheme 1. Synthetic approach of folate–PEG–PCL.

magnet purchased from Ningbo permanent magnetics Co., Ltd (China) (Dimension: $d = 18$ mm, $h = 15$ mm; field strength: ≈ 0.42 T) was used.

2.8. Dual targeting study

KB cells were seeded at 5×10^5 cells/well in 60 mm petri dish and maintained in 4 mL of RPMI-1640 medium supplemented with 10% heat-inactivated fetal bovine serum (FBS). After incubation for 24 h in a humidified incubator (37 °C, 5% CO_2) at 37 °C, a predetermined amount of micelles in PBS was added into each dish to adjust for a DOX concentration of 5 μg/mL. To evaluate the influence of magnetic field on cell uptake of micelles, a cylindrical sintered N-35 Nd–Fe–B magnet (Dimension: $d = 18$ mm, $h = 15$ mm; field strength: ≈ 0.42 T) was placed against the outer bottom wall of the petri dish at different distances (i.e. 0 cm, 1 cm and 2 cm, respectively) to vary the magnetic field strength applied to the cells. For the Prussian blue staining experiment, cells were incubated and then washed twice with PBS, fixed by adding 2 mL of 4% paraformaldehyde-containing PBS fixative solution for 30 min. Media in the dish were replaced with the same but fresh paraformaldehyde-containing PBS. Each dish received a 2.5 mL of a 2:1 (v/v) mixture of 2% potassium ferrocyanide(II) trihydrate and 2% HCl solutions, after which cells were incubated for 20 min at 37 °C. Cells were then washed three times with PBS, and the Prussian blue staining result and DOX fluorescence were assessed on a Nikon TE2000-U inverted fluorescence microscope. For the flow cytometry analysis, cells were incubated with 2 mL of RPMI-1640 medium (DOX concentration: 5 μg/mL). Afterwards, cells were washed with PBS, trypsinized, centrifuged, resuspended in 1 mL of PBS, and

analyzed via flow cytometry. For the control experiment in which free folate was added to compete with the folate-functionalized micelles, KB cells were first incubated with free folate (10 mM) for 1 h, and then co-incubated with folate-functionalized micelles for 0.5 h.

2.9. In vitro cytotoxicity against KB cells

KB cells were seeded onto 24-well plates with a seeding density of 10,000 cells per well, maintained in 1 mL RPMI-1640 medium supplemented with 10% inactivated FBS, and incubated for 1 day at 37 °C in a humidified atmosphere with 5% CO_2. Cells were then incubated in 1 mL RPMI-1640 medium containing DOX-loaded micelles (DOX concentration: 2.5 μg/mL) for 3 days. A 0.415 T magnetic field was applied to cells throughout the course of cell incubation. In control experiments, micelles loaded with SPIO alone were added to the culture media, and the cells were then incubated for 4 days. Afterwards, cells were washed twice with PBS, and incubated for 4 h in 1 mL RPMI-1640 medium containing 100 μL MTT (5 mg/mL in PBS). The precipitate was dissolved in 750 μL DMSO and analyzed on a BIO-RAD microplate reader.

2.10. Statistical analysis

All data were repeated three times in experiments and are reported as mean values with standard deviations. Statistical analysis was carried out using Student's *t*-test. Differences were considered statistically significant when $p < 0.05$.

3. Results and discussion

Amphiphilic block copolymers, folate–PEG–PCL ($M_n = 5.1$ kDa, M_n(PEG) = 2.9 kDa, M_n(PCL) = 0.87 kDa) and allyl-PEG–PCL ($M_n = 3.8$ kDa, M_n(PEG) = 2.9 kDa, M_n (PCL) = 0.87 kDa), were used for micelle fabrication. They were synthesized by multi-step chemical reactions as shown in Scheme 1. The polymer structure has been characterized and the molecular weight was determined by Gel permeation chromatography (GPC) in our recent publication [21]. GPC measurement indicated that the M_n of folate–PEG–PCL is 5.1 kDa. Hydrophobic SPIO nanoparticles, measuring ~6 nm in diameter, were synthesized with precise control of particle diameter (Fig. 1A). The selected area electron diffraction (SAED) pattern (inset in Fig. 1A) indicates that the particle composition is

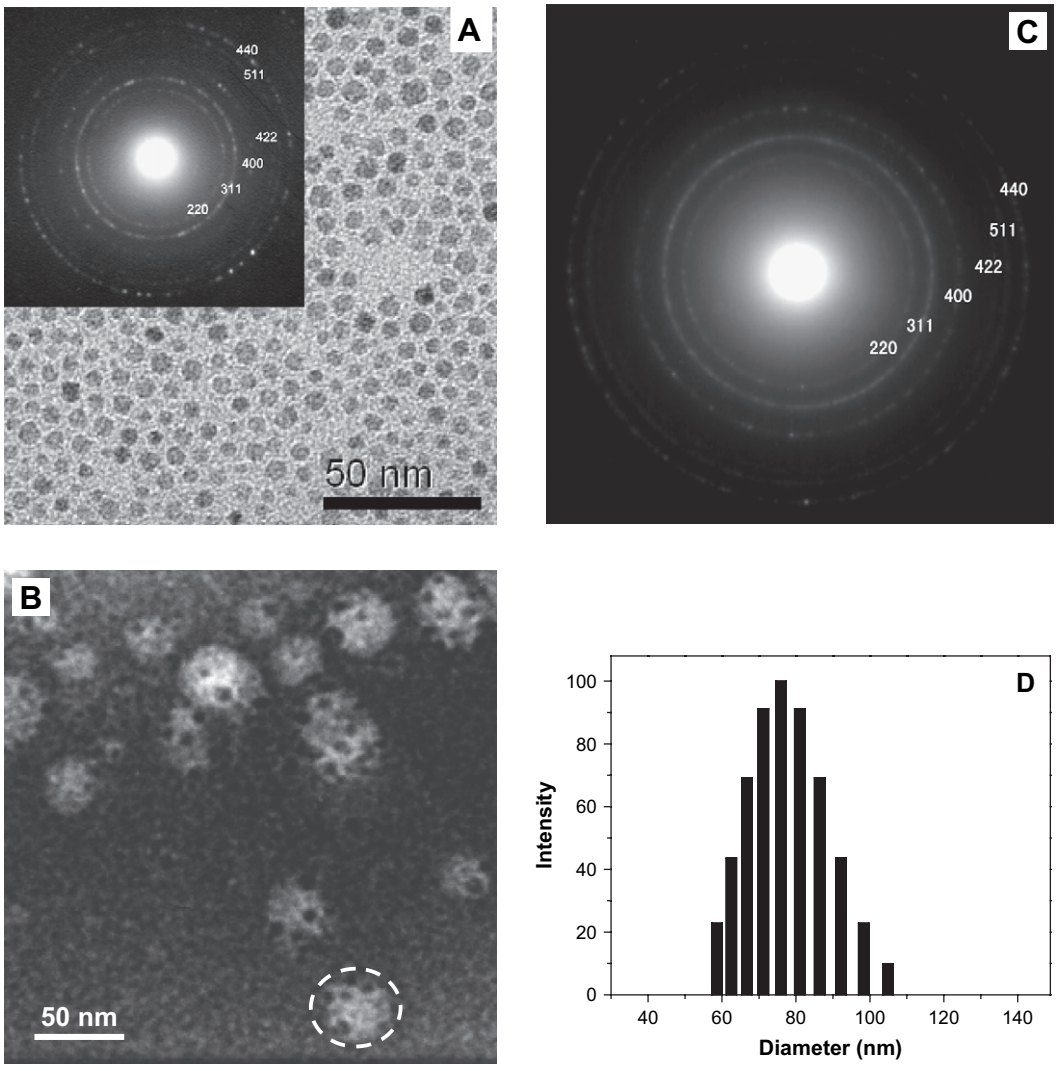

Fig. 1. Transmission electron microscopy (TEM) image of (A) 6 nm Fe_3O_4 nanoparticles; selected area electron diffraction (SAED) pattern (B); TEM image (C) and dynamic light scattering (DLS) histogram (D) of SPIO–DOX-loaded magnetic micelle based on folate–PEG–PCL copolymer. Sample for TEM measurement was negatively stained by 2% PTA. Inset in (A) shows the SAED pattern acquired from 6 nm Fe_3O_4 nanoparticles. As an example, one micelle particle was marked with a dashed white circle.

magnetite (Fe_3O_4) [4]. SPIO and anticancer drug DOX were jointly loaded into the targeting micelles, as shown in Scheme 2. The loading contents of SPIO and DOX in the micelles are summarized in Table 1. TEM image (Fig. 1C) of DOX and SPIO-loaded micelles shows that they are uniform in shape and size distribution, and SPIO particles were successfully encapsulated into micelles. Dynamic light scattering (DLS) measurements showed that the mean diameters were 29 ± 2 nm and 30 ± 2 nm for blank micelles (i.e. SPIO and DOX-free micelles), and 71 ± 1 nm and 75 ± 3 nm for SPIO and DOX-loaded micelles. The SPIO and DOX-loaded micelles showed a significant increase in size, mainly due to SPIO loading [23]. The SAED pattern of these magnetic micelles shows no difference from that of the 6 nm SPIO nanoparticles (Fig. 1B), indicating that SPIO nanoparticle has not changed its crystalline structure during the encapsulation process. Magnetization measurements also provided evidence that the SPIO nanoparticle encapsulated in micelles maintained its crystalline structure (Fig. 2). Both SPIO and micelles are superparamagnetic at room temperature, and the saturation magnetization (83.5Fe emu/g) of the magnetic micelles is slightly higher than that of SPIO (78.1Fe emu/g). At 10 K, both SPIO and SPIO-loaded micelles displayed ferromagnetic properties with a coercivity of 244 Oe for SPIO and 120 Oe for SPIO–DOX-micelles.

Release of DOX from SPIO–DOX-loaded micelles was pH-dependent, and loading of the SPIO nanoparticles within micelle core did not lead to an obvious change in the DOX-release profile. In control experiments, free DOX quickly diffused out of the dialysis bag at both pHs 7.4 and 5.0. The release of free DOX was completed in 3 h. As shown in Fig. 3, DOX release in the two media revealed a biphasic release pattern consisting of an initial burst release followed by a sustained and slow release over a prolonged time of up to several weeks. Within 2 weeks, SPIO loading did not obviously affect the release profile of DOX at pH 5. However, for time points after 15 days, faster DOX release occurs from SPIO–DOX-micelles compared to DOX-micelles. At pH 7.4, DOX release was relatively slow for both formulations, with less than 10 wt.% of DOX released

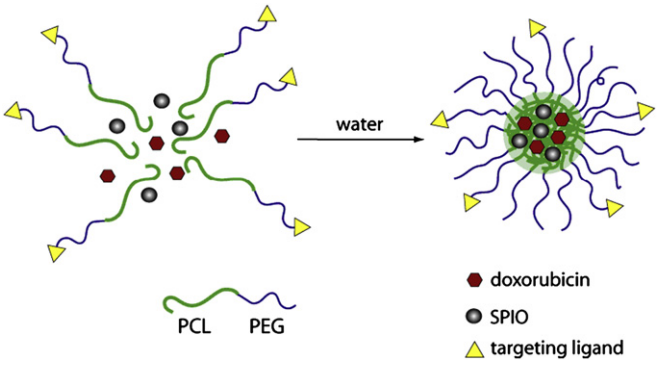

Scheme 2. Formation of SPIO–DOX-encapsulated micelles.

Table 1
Micelle size, SPIO and DOX loading densities

Micelle formulation	Micelle diameter (nm)	SPIO loading (wt.%)	DOX loading (wt.%)	
Allyl-PEG–PCL	SPIO–DOX-free micelle	30 ± 2.0	–	–
	SPIO-free micelle	33 ± 1.0	–	2.5 ± 0.1
	SPIO–DOX-micelle	71 ± 1.0	12.2 ± 2.4	2.7 ± 0.3
Folate–PEG–PCL	SPIO–DOX-free micelle	29 ± 2.0	–	–
	SPIO-free micelle	30 ± 1.0	–	3.0 ± 0.1
	SPIO–DOX-micelle	75 ± 3.0	10.2 ± 2.1	2.8 ± 0.2

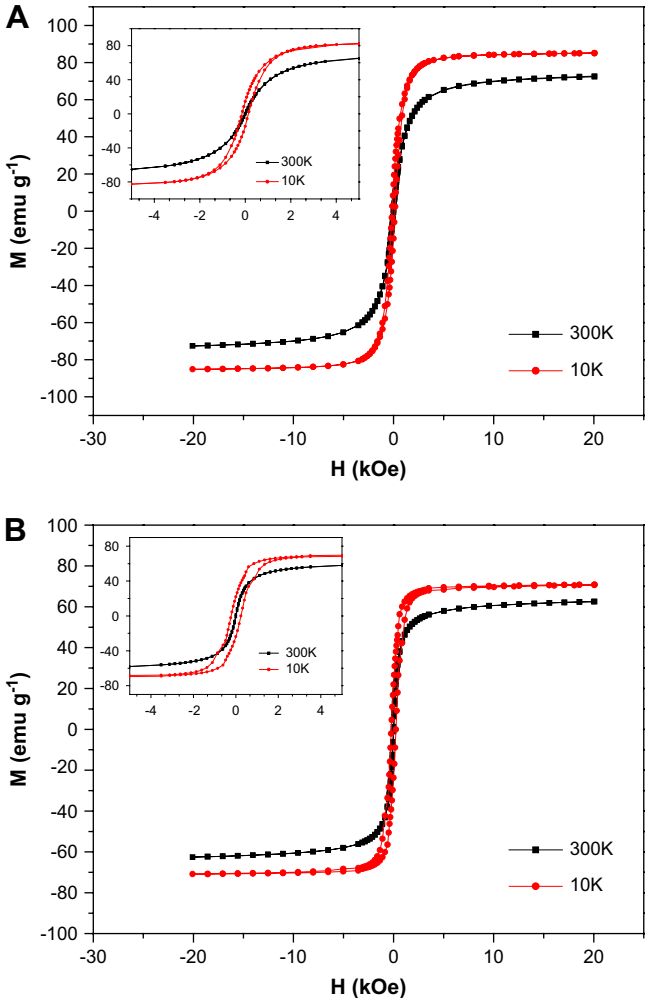

Fig. 2. Hysteresis loops of SPIO–DOX-micelle based on allyl-PEG–PCL (A) and 6 nm Fe_3O_4 nanoparticles (B) measured at 300 K and 10 K. The two insets in the figure show the local magnification.

in 5 days, and only 18 wt.% of DOX released after 35 days for both micellar formulations. DOX release at pH 5.0 was much faster than that at pH 7.4 from both formulations, with the difference in release being statistically significant. More than 30 wt.% and 70 wt.% of DOX was released in 5 and 35 days, respectively. It is likely due to the re-protonation of the amino group of DOX and faster degradation of micelle core at lower pH, and this type of faster release of DOX in acidic conditions was also observed by Kataoka and coworkers with the DOX-loaded polymeric micelles [2b]. This observed pH-dependent DOX release behavior is hypothesized to potentiate drug release from micelles once the micelles enter the tumor cells via endocytosis and are trapped within acidic endosomal compartments.

The magnetic responsiveness of SPIO nanoparticles and SPIO–DOX-micelles in solution was visualized by a simple experiment in which a 0.42 T magnet was placed near the glass vials (Fig. 4). Both SPIO nanoparticles in hexane and SPIO–DOX-micelles in water deposited notably on the wall adjacent to the magnet within 30 s. These observations provide direct evidence that SPIO–DOX-micelles, like SPIO nanoparticles, possess prompt responsiveness to an external magnetic field. In addition, we can easily deduce that DOX and SPIO were coencapsulated successfully into the micelle core based on the fact that the SPIO–DOX-micelle solution became transparent and colorless due to the magnetically induced separation of micelles from solution. Magnetic micro-devices such as

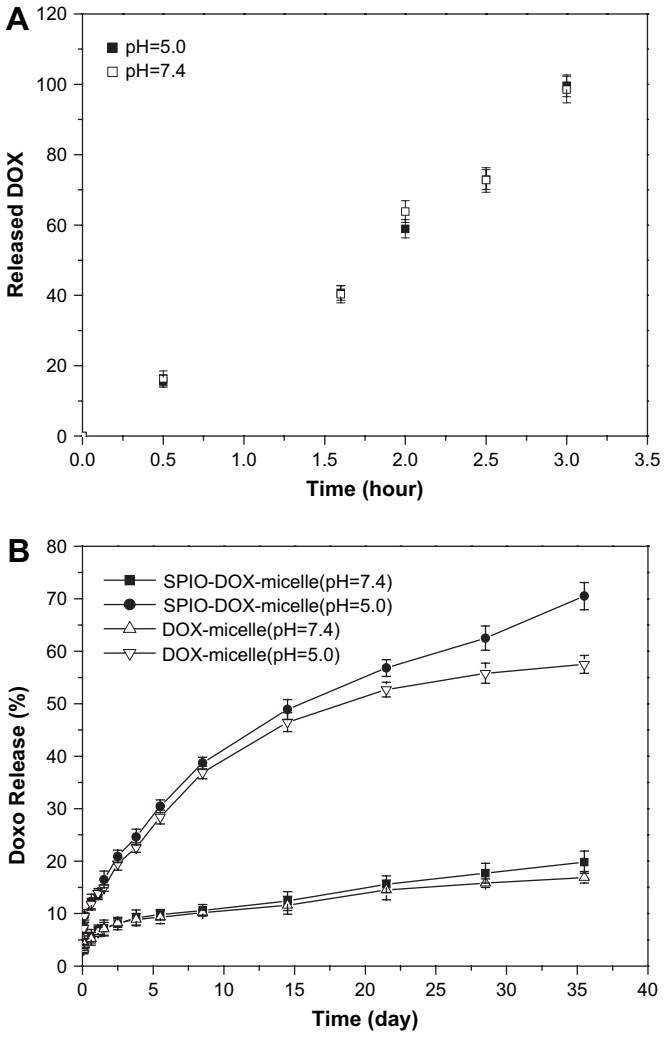

Fig. 3. (A) Release profiles of free DOX from solutions at pH 5.0 and pH 7.4. (B) In vitro DOX-release profiles from micelles based on folate–PEG–PCL at neutral (pH 7.4) and acidic conditions (pH 5.0) at 37 °C. Data are presented as mean ± SD ($n = 3$).

magnetic nanotubes and silica coated nanoparticles have demonstrated potential in magnetic-field assisted bio-separation and cell sorting in addition to specific targeting applications [24,25]. Our experiments served to highlight the potential of using an easy and effective way to direct drug-loaded nanoparticles from a solution to the targeted locations under an external magnetic field. In particular, the magnetic micelles developed herein are highly sensitive to external magnetic field and thus have potential as a magnetically guided nanoplatform for drug delivery.

As a proof of concept, we designed simple in vitro cell culture experiments to test the dual magnetic and folate targeting effects of SPIO–DOX-loaded micelles. The experimental design is shown in Fig. 5. A commercially available 0.42 T Nd–Fe–B magnet was placed against the outer bottom surface of the petri dish, and the large black circle shows the position of the magnet. Cells in two locations within the petri dish, referred to as circle 1 and 2 areas, were investigated regarding DOX fluorescent intensity and Prussian blue staining. Circle 1 is within the black circle showing the magnet position and thus is in the strongest magnetic field, while the magnetic field applied to circle 2 is much weaker. As visualized under microscopy, both Prussian blue and DOX fluorescence intensities indicate that cells located inside circle 1 have taken up considerably more folate-functionalized and SPIO–DOX-loaded micelles than cells located inside circle 2 after 3 h incubation (see Fig. 5A *vs* B for Prussian blue, and C *vs* D for fluorescence images). To evaluate the effect of magnetic field strength on cell uptake, we vertically positioned the magnet at different distances from the dish bottom at 0 cm, 1 cm, and 2 cm. The magnetic field strengths applied to the cells in circle 1 in three magnet positions are 4150 G, 1280 G and 450 G, respectively, as measured with a LakeShore 421 gaussmeter. We incubated the cells with folate-encoded and folate-free SPIO–DOX-loaded micelles in the presence of the external magnetic field to further compare the magnetic and molecular targeting effects. After 0.5 h cell incubation time with micelle-containing media in varied magnetic field strengths, DOX fluorescence of cells was analyzed with inverted fluorescence microscopy and flow cytometry to investigate the cell uptake level of micelles. Fig. 6A and B shows the DOX fluorescence images and quantitative fluorescence intensity of cells from circle 1. Two major findings were observed: first, a strong magnetic field has a considerable

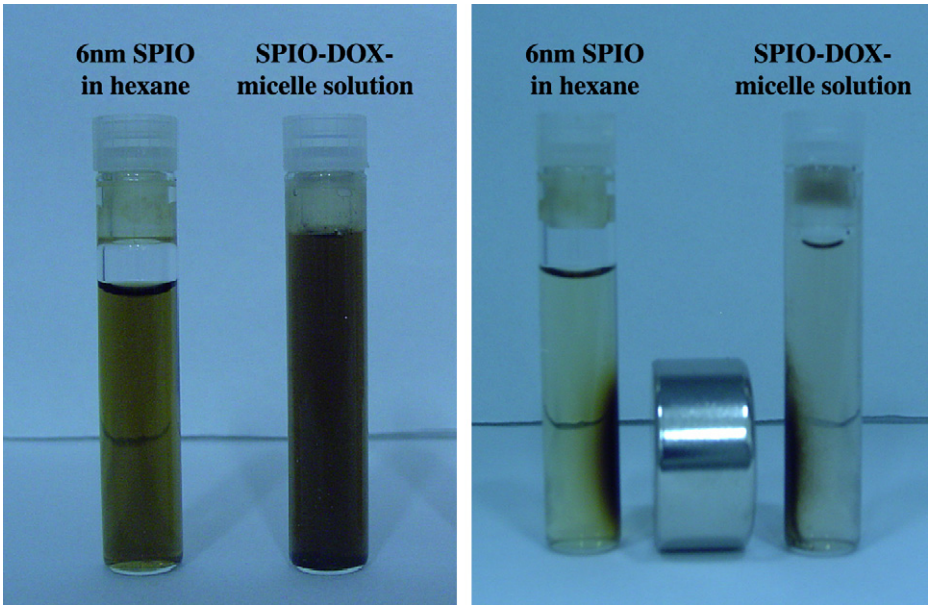

Fig. 4. Samples before and after imposing an external magnetic field. Micelles based on folate–PEG–PCL.

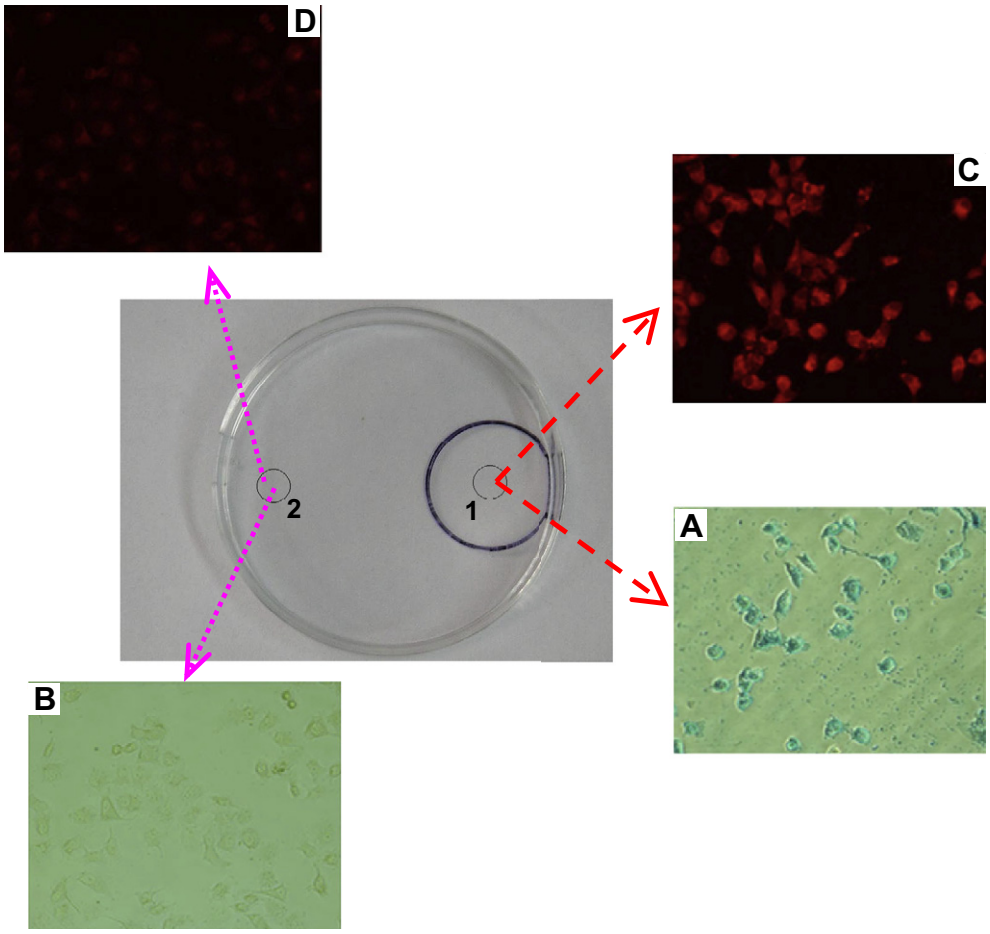

Fig. 5. Micrographs of SPIO–DOX-loaded micelles based on folate–PEG–PCL after 3 h incubation in an external magnetic field. (A) and (B) refer to the Prussian blue staining of cells located in circle 1 and circle 2; (C) and (D) refer to the DOX fluorescent intensity of cells located in circle 1 and circle 2. Circle 1 and circle 2 indicate the different positions of magnet, respectively. Determined magnetic field strength: 4150 G for cycle 1; 150 G for cycle 2.

influence on the cell uptake of the magnetic micelles. The relative fluorescence intensity of cells as determined by flow cytometry decreased 84% and 92%, respectively, for folate-encoded and folate-free micelles when the magnetic field strength was decreased to 0 G from 4150 G. At high magnetic field strength (i.e. 4150 G), the magnetic targeting effect is more apparent than that from folate targeting. In comparison, at the weaker magnetic field strength (450 G), data show no obvious magnetic-induced targeting effect on the cell uptake of micelles. Hence, we conclude from this experiment that the strong external magnetic field can effectively increase the local concentration of micelles in media near the investigated cells. Additionally, folate-mediated cell targeting became much more evident when the external magnetic field was weakened. As shown in Fig. 6B, folate targeting in a 4150 G magnetic field led to a 1.2-fold increase in DOX fluorescence in cells, while the same targeting resulted in an increase by a factor of 2.3 and 2.4 in 450 G and 0 G magnetic fields, respectively. Similar results can be observed via fluorescence microscopy analysis as well (Fig. 6A). The fluorescence disparity between the samples demonstrated the dynamic interplay of magnetic targeting *vs* biological targeting via folate under different experimental conditions. In the ligand competing assay at 0 G magnetic field, cell uptake of targeting micelle dropped back to almost the same level of folate-free micelle when large amount of free folate (10 mM) was present in the cell culture medium.

The potential of these Fe_3O_4-loaded and folate-encoded micelles as a novel drug delivery platform was further demonstrated by the MTT cytotoxicity assay. Two groups of experimental controls, micelles without DOX and SPIO loaded inside as well as micelles loaded with SPIO alone, did not show significant cell growth inhibition, indicating minimal cell cytotoxicity of DOX-free micelles. The cytotoxicity of four DOX-loaded micelles with or without magnetic responsiveness was compared in order to further verify the dual targeting effect. The external magnetic field strength applied to cells during the course of cell incubation was set to 4150 G. As shown in Fig. 7, after 3 days cell incubation in the given magnetic field, four micelles exhibited significantly different cytotoxicities in KB cells. Although magnetic targeting resulted in an ideal cell growth inhibition even for the non-folate magnetic micelle, the best outcome (i.e. $9 \pm 3\%$ cell viability) was achieved with folate-encoded and Fe_3O_4-loaded micelles. Furthermore, in the two micelles without Fe_3O_4 loading, folate targeting showed increased cytotoxic effects, with cell viabilities consisting of $77 \pm 2\%$ and $57 \pm 3\%$ for the folate-free and the folate-encoded micelles, respectively ($p < 0.05$). It is noteworthy that as a whole, these two DOX-encapsulated micelle formulations without magnetic responsiveness were much less effective in cell growth inhibition. These MTT cytotoxicity data are in agreement with results obtained in the cell uptake study, and revealed once more the dual targeting effect of Fe_3O_4-loaded and folate-encoded micelles to target cells in the presence of a strong external magnetic field. In the dual targeting strategy, the external magnetic field will first guide the accumulation of micelles to tumor tissues after which a targeting ligand would allow for binding to the cell membrane receptors to facilitate micelle uptake inside tumor cells. Animal experiments are currently in progress to evaluate the efficacy of this dual targeting micelle *in vivo*.

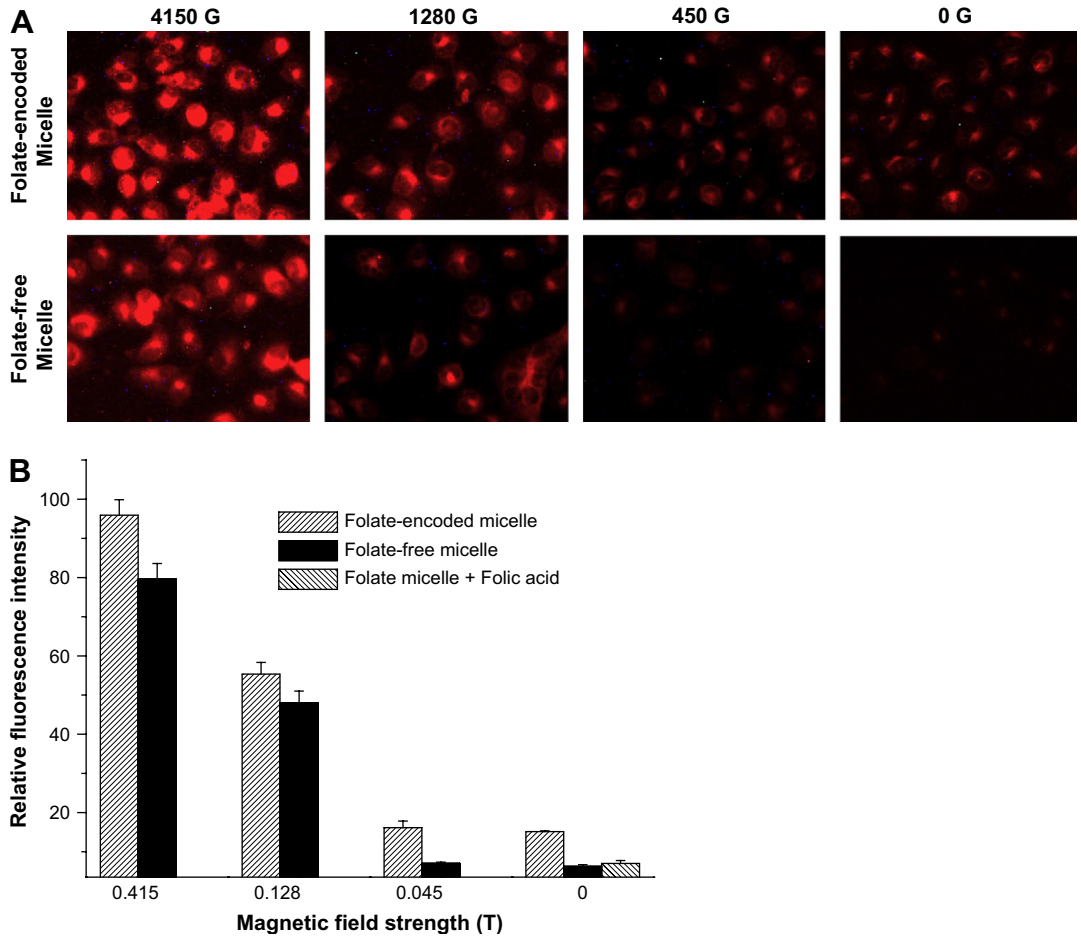

Fig. 6. Fluorescence microscopy images (A) and flow cytometry data (B) for KB cells upon treatment with the SPIO–DOX-loaded micelles in different magnetic field strengths. Relative fluorescence intensities obtained in flow cytometry are presented as mean ± SD ($n = 3$). Cell incubation time: 0.5 h. Folate competing assay was performed in the presence of large amount of free folate (10 mM) in solution. $p < 0.05$ for all data points when comparing between folate-encoded and folate-free micelles.

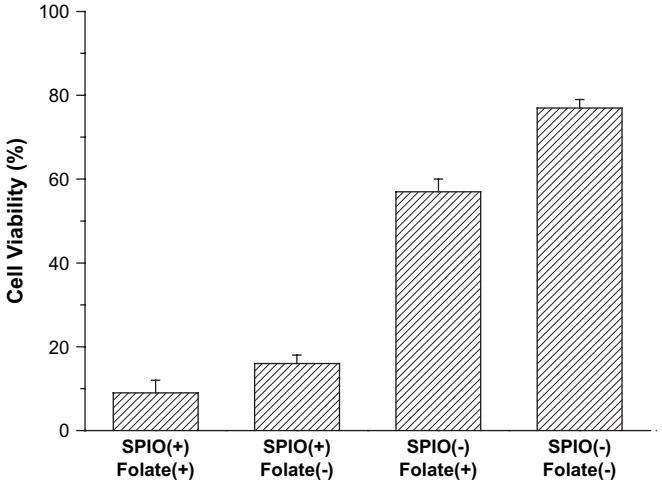

Fig. 7. (A) Cytotoxicity of four DOX-encapsulated micelle formulations with or without magnetic responsiveness. Cells were incubated for 3 days in micelle-containing media (DOX concentration: 2.5 μg/μL), and an external magnetic field (0.415 T) was applied to cells during the whole course of cell incubation. Micelle characteristics are shown below the *X*-axis as follows: SPIO (+) and SPIO (−) for micelles with and without SPIO loading, while folate (+) and folate (−) for micelles with and without folate functionalization. For example, under such denotation, SPIO (+) and folate (+) together indicate SPIO-loaded and folate-encoded micelles. Data are presented as mean ± SD ($n = 3$).

4. Conclusions

In summary, we report a novel dual targeting strategy to maximize drug delivery efficacy to tumor cells. A nanoscale, micellar carrier from a block copolymer, folate–PEG–PCL, has been developed to encapsulate superparamagnetic Fe_3O_4 and to deliver an anticancer drug, doxorubicin. These micelles demonstrate the potential to achieve dual tumor targeting (i.e. magnetic field-guided and ligand-directed targeting) of micelles to tumor cells. The dual targeting strategy opens up several opportunities for enhancing drug delivery efficiency and cancer specificity during chemotherapy.

Acknowledgement

This work was supported by the National Natural Science Foundation of China (Grant Nos. 20474076, 20728403 and 50673103).

References

[1] (a) Xiong DA, He ZP, An YL, Zhe Li, Wang H, Chen X, et al. Polymer 2008;49:2548–52;
(b) Kim SY, Shin G, Lee YM. Biomaterials 1999;20:1033–42.
[2] (a) Li JB, Shi LQ, An YL, Li Y, Chen X, Dong HJ. Polymer 2006;47:8480–7;
(b) Kataoka K, Matsumoto T, Yokoyama M, Okano T, Sakurai Y, Fukushima S, et al. J Controlled Release 2000;64:143–53;
(c) Liu DH, Zhong CL. Polymer 2008;49:1407–13.

[3] (a) Chen C, Yu CH, Cheng YC, Yu PHF, Cheung MK. Biomaterials 2006;27:4804–14;
(b) Huynh DP, Shim WS, Kim JH, Lee DS. Polymer 2006;47:7918–26.
[4] Ai H, Flask C, Weinberg B, Shuai X, Pagel MD, Farrell D, et al. Adv Mater 2005;17:1949–52.
[5] Savic R, Luo L, Eisenberg A, Maysinger D. Science 2003;300:615–8.
[6] (a) Hu YQ, Kim MS, Kim BS, Lee DS. Polymer 2007;48:3437–43;
(b) Kataoka K, Harada A, Nagasaki Y. Adv Drug Delivery Rev 2001;47:113–31.
[7] Sutton D, Nasongkla N, Blanco E, Gao J. Pharm Res 2007;24:1029–46.
[8] Licciardi M, Giammona G, Du JZ, Armes SP, Tang YQ, Lewis AL. Polymer 2006;47:2946–55.
[9] Nasongkla N, Shuai X, Ai H, Weinberg BD, Pink J, Boothman DA, et al. Angew Chem 2004;116:6483–7.
[10] Daniels TR, Delgado T, Helguera G, Penichet ML. Clin Immunol 2006;121:159–76.
[11] Dinauer N, Balthasar S, Weber C, Kreuter J, Langer K, Briesen HV. Biomaterials 2005;26:5898–906.
[12] Widder KJ, Senyei AE, Scarpelli DG. Proc Soc Exp Biol Med 1978;58:141–6.
[13] Widder KJ. Proc Natl Acad Sci USA Biol Sci 1981;78:579–81.
[14] Alexiou C, Arnold W, Klein RJ, Parak FG, Hulin P, Bergemann C, et al. Cancer Res 2000;60:6641–8.
[15] Häfeli UO. Int J Pharm 2004;277:19–24.
[16] Alexiou C, Jurgons R, Schmid R, Hilpert A, Bergemann C, Parak F, et al. J Magn Magn Mater 2005;293:389–93.
[17] Lübbe AS, Bergemann C, Riess H, Schriever F, Reichardt P, Possinger K, et al. Cancer Res 1996;56:4686–93.
[18] Schillinger U, Brill T, Rudolph C, Huth S, Gersting S, Krötz F, et al. J Magn Magn Mater 2005;293:501–8.
[19] Rudge SR, Kurtz TL, Vessely CR, Catterall LG, Williamson DL. Biomaterials 2000;21:1411–20.
[20] Nasongkla N, Bey E, Ren J, Ai H, Khemtong C, Guthi JS, et al. Nano Lett 2006;6:2427–30.
[21] Yang X, Deng W, Fu L, Gao J, Quan D, Shuai X. J Biomed Mater Res A 2008;86A:48–60.
[22] Sun S, Zeng H, Robinson DB, Raoux S, Rice PM, Wang SX, et al. J Am Chem Soc 2004;126:273–9.
[23] Shuai X, Ai H, Nasongkla N, Kim S, Gao J. J Controlled Release 2004;98:415–26.
[24] Yoon TJ, Yu KN, Kim E, Kim JS, Kim BG, Yun SH, et al. Small 2006;2:209–15.
[25] Son SJ, Reichel J, He B, Schuchman M, Lee SB. J Am Chem Soc 2005;127:7316–7.